Biochemistry and Biophysics Reports 40 (2024) 101822

Contents lists available at ScienceDirect

Biochemistry and Biophysics Reports

journal homepage: www.elsevier.com/locate/bbrep

Altered fatty acid distribution in lysosome-associated membrane protein-2 deficient mice

Ziming Xu [a], Shoji Notomi [a,*], Guannan Wu [a], Yosuke Fukuda [a], Yusuke Maehara [a], Masatoshi Fukushima [a], Yusuke Murakami [a], Masatomo Takahashi [b], Yoshihiro Izumi [b], Koh-Hei Sonoda [a]

[a] Department of Ophthalmology, Graduate School of Medical Sciences, Kyushu University, 3-1-1 Maidashi, Higashi-Ku, Fukuoka, 812-8582, Japan
[b] Division of Metabolomics, Medical Research Center for High Depth Omics, Medical Institute of Bioregulation, Kyushu University, Fukuoka, 812-8582, Japan

ARTICLE INFO

Keywords:
Fatty acid metabolism
Lipidomics
PC
TGs
LC-MS
PUFA

ABSTRACT

Lysosome-associated membrane protein-2 (LAMP2) deficiency causes the human Danon disease and represents a lysosomal dysfunction because of its pivotal role in regulating autophagy and lysosome biogenesis. LAMP2-deficient mice exhibit a spectrum of phenotypes, including cardioskeletal myopathy, mental retardation, and retinopathy, similar to those observed in patients with Danon disease. Its pathology is thought to involve altered energy metabolism and lipid dysregulation; however, the lipidomic profiles of LAMP2-deficient animals have not been investigated. In this study, we investigated lipid alterations in LAMP2 KO mice tissues, including those of the liver, plasma, and retina, using liquid chromatography-mass spectrometry. Our results revealed significantly increased free fatty acid (FFA) levels and decreased in triglyceride (TG) levels in LAMP2 KO liver tissues at three and six months. Phosphatidylcholine (PC) and phosphatidylethanolamine (PE) species significantly decreased in LAMP2 KO mice livers at six months. Similarly, plasma TG and PC/PE levels decreased in LAMP2 KO mice. In contrast, plasma FFA levels were significantly lower in LAMP2 KO mice. Retina FFA levels were elevated in LAMP2 KO mice, accompanied by a partial decrease in PC/PE at six months. In summary, FFA levels increased in several tissues but not in the LAMP2 KO mice plasma, suggesting the potential consumption of FFA as an energy source in the peripheral tissues. The depletion of TG and PC/PE accelerated with age, suggesting an underlying age-dependent energy crisis condition. Our findings underscore the dysregulated distribution of fatty acids in LAMP2-deficient animals and provide new mechanistic insights into the pathology of Danon disease.

1. Introduction

Lysosome-associated membrane protein-2 (LAMP2), a highly glycosylated protein in lysosomal membranes, plays a critical role in lysosomal biogenesis and autophagosome/phagosome maturation [1]. In humans, LAMP2 deficiency leads to Danon disease (DD), a rare lysosomal storage disorder characterized by cardiomyopathy, skeletal myopathy, and mental retardation [2]. Patients with DD can also present with symptomatic or asymptomatic retinopathy [3]. LAMP2 knockout (L2KO) mice have been extensively studied to understand DD pathology [4]. Similar to characteristics observed in patients with DD, L2KO mice exhibit autophagic vacuole accumulation in several tissues, including the liver, pancreas, spleen, kidney, and skeletal and heart muscles [4]. L2KO mice show increased mortality between postnatal days 20 and 40; the surviving mice are fertile and have an almost normal lifespan [4].

Furthermore, L2KO mice have been demonstrated to exhibit various metabolic dysfunctions, suggesting the significant role of LAMP2 in autophagy, energy balance maintenance, and metabolic stability. The liver-specific elimination of LAMP2A, a major LAMP2 isoform, in mice alters carbohydrate metabolism, dysregulating the energy balance [5]. LAMP2 deficiency also causes abnormalities in cholesterol trafficking, characterized by the accumulation of unesterified cholesterol in late endosomes and lysosomes [6]. In the central nervous system, L2KO mice have been shown to exhibit lipid storage in hippocampal neurons and their presynaptic terminals [7]. For mechanistic insights into retinopathy in DD, our previous study demonstrated that L2KO mice developed

* Corresponding author. Department of Ophthalmology, Graduate School of Medical Sciences, Kyushu University, 3-1-1 Maidashi, Higashi-Ku, Fukuoka, 812-8582, Japan.
E-mail address: noutomi.shouji.926@m.kyushu-u.ac.jp (S. Notomi).

https://doi.org/10.1016/j.bbrep.2024.101822
Received 1 July 2024; Received in revised form 29 August 2024; Accepted 2 September 2024
Available online 5 September 2024
2405-5808/© 2024 Published by Elsevier B.V. This is an open access article under the CC BY-NC-ND license (http://creativecommons.org/licenses/by-nc-nd/4.0/).

retinal degeneration, associated with a delayed digestion of photoreceptor outer segments and a dysregulated autophagic flux in the retinal pigment epithelium [8]. Moreover, aged L2KO mice exhibited basal laminar deposit formation, an important histopathological feature of age-related macular degeneration, which is the leading cause of blindness in developed countries [8–10]. Additionally, LAMP2 deficiency impairs the improvement in glucose tolerance induced by intermittent fasting in mice, highlighting its important role in glucose metabolism [11]. Collectively, LAMP2 deficiency may cause the dysregulation of energy and lipid metabolism; however, a comprehensive lipidomic analysis of L2KO mice has not been performed. Hence, we aimed to investigate the composition of fatty acids using liquid chromatography-tandem mass spectrometry (LC-MS/MS) to compare L2KO and wild-type (WT) mice in the liver, plasma, and retina. Our results indicated that the proportion and distribution of free fatty acids (FFA), phosphatidylcholine (PC), phosphatidylethanolamine (PE), and triglycerides (TGs) [11], significantly changed in L2KO mice with age.

2. Materials and methods

2.1. Animals

All experiments were performed in adherence with the declaration of Helsinki, were approved by the Animal Care Committee of the Institute of Medical Science, Kyushu University (approval number: #A23-002-2), and were conducted in accordance with the Association for Research in Vision and Ophthalmology Statement for the Use of Animals in Ophthalmic and Vision Research. The animal data have been reported in adherence with the Animal Research: Reporting of In Vivo Experiments (ARRIVE) guidelines. For the experiments, adult male LAMP2 KO mice (LAMP2 y/-) and their WT littermates (LAMP2 y/+) were selected at the age of three or six months. LAMP2 KO mice, originally generated in Prof. Saftig's lab, were backcrossed with C57BL6J mice for at least five generations. The mice were placed in a 12-h light/dark environment (8:00 a.m. to 8:00 p.m.) with ad libitum access to normal chow (5058 laboratory rodent diet 20, LabDiet, MO, USA) and water in the animal facility of Kyushu University.

2.2. Preparation of mice tissues

The liver, retina, and plasma from three or six-month-old male L2KO or WT sacrificed mice were collected (n = 4 mice per group). The liver, blood, or eyeballs were collected immediately after the mice were euthanized by cervical dislocation. Blood was collected in tubes containing the anticoagulant EDTA-2K. Plasma was separated by centrifugation at 3000×*g* for 15 min. The plasma volume and liver weights were measured. Retinas were extracted following a circumferential incision around the ora serrata and removal of the lens/vitreous.

The tissues were frozen in liquid nitrogen and crushed using a multibead shocker. To the liver and retina crush (powder), 700 μl of water was added, mixed well, and the homogenate was transferred to a glass test tube. After that, 2 mL methanol was quickly added and mixed to stop the metabolic enzyme reaction. The powder remaining in the multibead shocker was washed with 300 μL water and transferred to a test tube. For the plasma sample, 100 μL of serum was taken in a glass test tube and mixed with 900 μL water and 2 mL methanol. To all the test tubes, 2 mL of chloroform was added (5 mL in total) and shaken 10 min in a shaker. The tubes were centrifuged at 1000×*g* for 15 min at room temperature. A 100 μL of the lower layer was collected, 1/4 volume of the internal standard (25 μL) was added to it and was subjected to LC-MS/MS Lipidomic analysis. Multiple internal standards consisted of isotopes of lipids and lipids not present in specimens were used to correct retention times for the target compounds.

2.3. Lipidomic analysis using LC-MS/MS

LC-MS/MS experiments were performed by LSI Medience Corporation (Japan, Tokyo) using an Agilent 1260 Infinity II UPLC system equipped with a 6546 Quadrupole Time-of-Flight system (Agilent Technologies, USA, California) and operated by a Mass Hunter Workstation, as previously described [12].

2.4. Data analysis

Raw data were obtained from the mass spectrometer, including *m/z*, retention time, and intensity, and they were processed and analyzed as previously done [12].

2.5. Lipid classification

According to the definition that polyunsaturated fatty acids (PUFA) are fatty acids containing two or more double bonds [13], PC/PE with three or more double bonds were classified as PUFA-PC/PE because they contained at least one fatty acid with two or more double bonds. Otherwise, they were categorized as non-PUFA-PC/PE. Similarly, TGs with four or more double bonds were categorized as PUFA-TGs.

3. Statistics

Statistical differences between the two groups were analyzed using Student's *t*-test. Statistical significance was set at $P < 0.05$. Heatmaps were created using the online software Bioladder (https://www.bioladder.cn).

4. Results

4.1. Lipidomic analysis in the liver

First, we performed a lipidomic analysis of the liver, comparing L2KO and WT mice, as it is the primary organ regulating lipid transport and metabolism. This includes processes such as uptake, esterification, oxidation, and fatty acid secretion [14].

4.1.1. FFA (young liver)

LC-MS/MS analysis indicated that L2KO mice exhibited significant changes compared to the WT mice at a young age (three months) in the eight detected FFA species (Fig. 1A–B). All detected FFA species in the liver increased in L2KO mice compared to WT (Fig. 1C). Note that all the detected FFAs, except for myristic acid (14:0), increased by more than 2-fold.

4.1.2. TG (young liver)

In contrast, most TG species (47 out of 52) significantly decreased in L2KO mice compared to WT (Fig. 1A–B). We classified TGs with three or more double bonds as PUFA-TGs. Among the 52 TG species detected in the liver, 28 and 24 were classified as PUFA-TGs and non-PUFA-TGs, respectively (Fig. 1D). Both groups showed significant decreases: 92.9 % (26/28) of PUFA-TGs and 87.5 % (21/24) of non-PUFA-TGs. However, we observed that the decrease in PUFA-TGs became relatively less detectable as the number of double bonds increased.

4.1.3. PC/PE (young liver)

The changes in PC/PE species in young livers were less pronounced compared to those in TGs (Fig. 1A–B). We detected 43 PC/PE species, comprising 25 PUFA-PC/PE and 18 non-PUFA-PC/PE species; PC/PE species containing two or more double bonds were classified as PUFA-PC/PEs. Among non-PUFA-PC/PEs, 10 of 18 species showed (55.6 %) increased levels, whereas 4 out of 18 species (22.2 %) decreased (Fig. 1E, left panel), indicating their altered distributions. In contrast, PUFA-PC/PEs showed fewer changes compared to non-PUFA-PC/PEs,

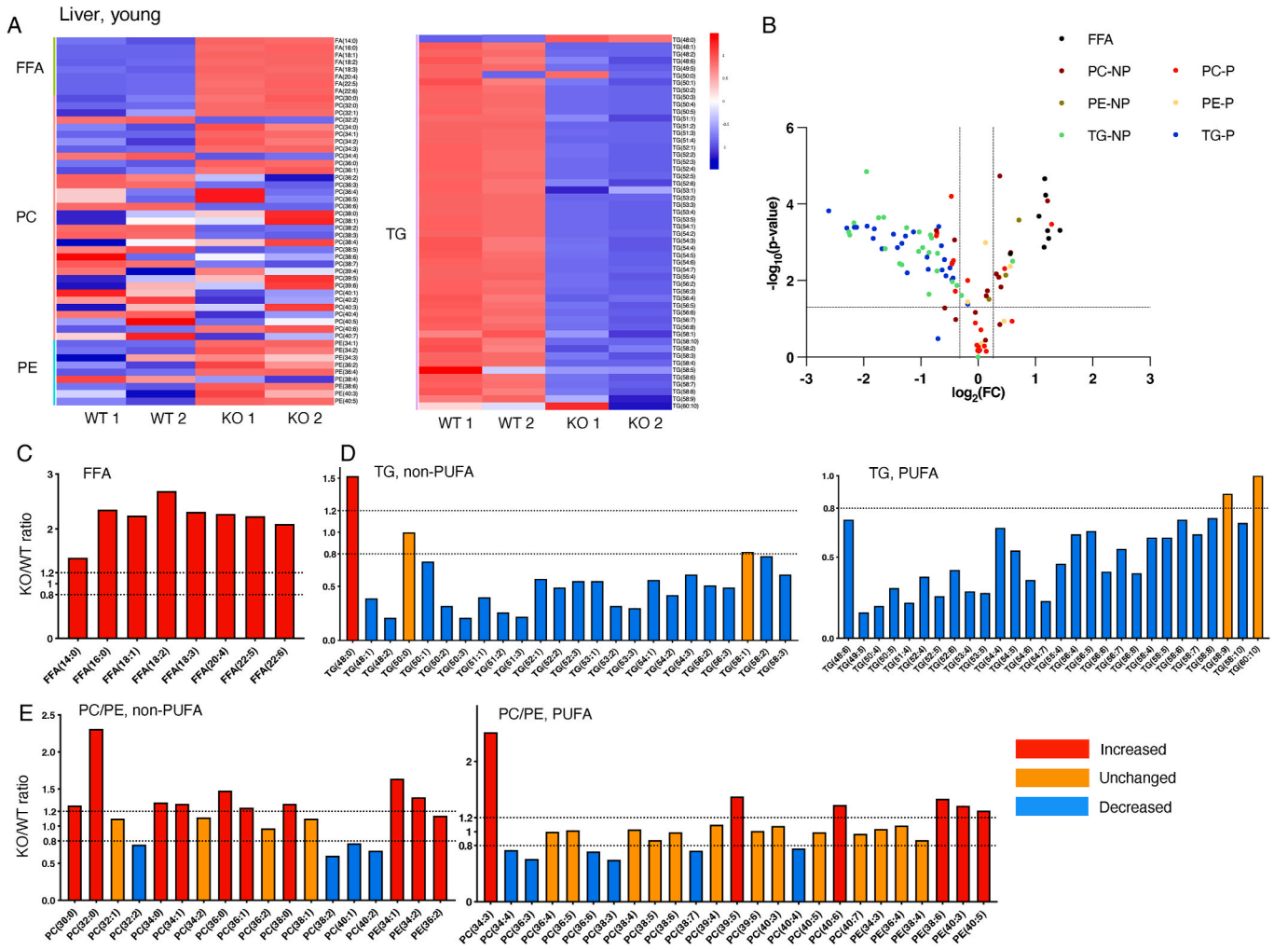

Fig. 1. Lipidomic analysis in young mice livers from WT and L2KO mice
Livers were extracted from three-month-old mice and analyzed using LC-MS/MS. A: Heatmap of all the lipids tested. All data were subjected to log transformation (base 10), mean-centered, and divided by the standard deviation of each variable. B: The volcano map of lipids classified based on unsaturation levels. Vertical dashed lines indicate fold-changes of 0.8 or 1.2, and the horizontal dashed lines indicate P = 0.05 based on Student's *t*-test. C–E: Fold changes of each FFA (C), non-PUFA-TG (D, left panel), PUFA-TG (D, right panel), non-PUFA-PC/PE (E, left panel), and PUFA-PC/PE (E, right panel). NP: non-PUFA; P: PUFA. FFA, free fatty acid; LAMP2, Lysosome-associated membrane protein-2; LC-MS/MS, liquid chromatography-tandem mass spectrometry; L2KO, LAMP2 knockout; PC, phosphatidylcholine; PE, phosphatidylethanolamine; PUFA, polyunsaturated fatty acid; WT, wild-type.

with 6 out of 25 (24 %) increasing and 6 out of 25 (24 %) decreasing (Fig. 1E, right panel). Therefore, phospholipid metabolism was less affected by LAMP2 deficiency at a young age compared to FFA or TG.

Collectively, lipid metabolism in the liver of young L2KO mice underwent significant alterations, particularly in TG and FFA, whereas changes in PC/PE were relatively less detectable at the age of three months.

4.1.4. FFA (old liver)

Based on previous findings that LAMP2 deficiency worsened with age [2], we examined liver samples from six-month-old L2KO and WT mice. Similar trends of increased FFA levels were observed in old livers of L2KO mice (Fig. 2A–B). We detected 10 FFA species in the old liver. The ratios of FFAs between L2KO and WT livers increased more significantly compared to those at a younger age (Fig. 2C). Pentadecanoate (15:0), linoleate (18:2), linolenic acid (18:3), and docosahexaenoic acid (DHA) (22:6) increased by more than 3-fold in the liver of old L2KO mice.

4.1.5. TG (old liver)

TGs in the liver of old L2KO mice exhibited more pronounced decreases compared to those in younger animals. In the aged liver, 52 TG species were detected, comprising 26 PUFA-TG species and 26 non-PUFA-TG species (Fig. 2B–D). The TG reductions in the old L2KO mice livers were more prominent compared to those in younger mice. Several PUFA-TGs, such as TG (52:5) and TG (54:7), decreased to less than 10 % of their levels in WT mice. This depletion of TGs in old L2KO mice suggests that TGs may be catabolized for persistent energy consumption because of the LAMP2 deficiency.

4.1.6. PC/PE (old liver)

While changes in PC/PE in young L2KO mice livers were variable, PC/PEs significantly reduced in the old L2KO mice livers. Among the 39 PC/PE species detected, 23 were PUFA-PC/PEs and 16 were non-PUFA-PC/PEs (Fig. 2E). We observed 56.3 % (9/16) of non-PUFA-PC/PE species and 91.3 % (21/23) of PUFA-PC/PE species to have shown reductions. Note that this decreasing trend in PC/PEs was not evident in the young mice livers.

4.2. Lipidomic analysis in the plasma

Next, lipidomic analysis was performed on mouse plasma according

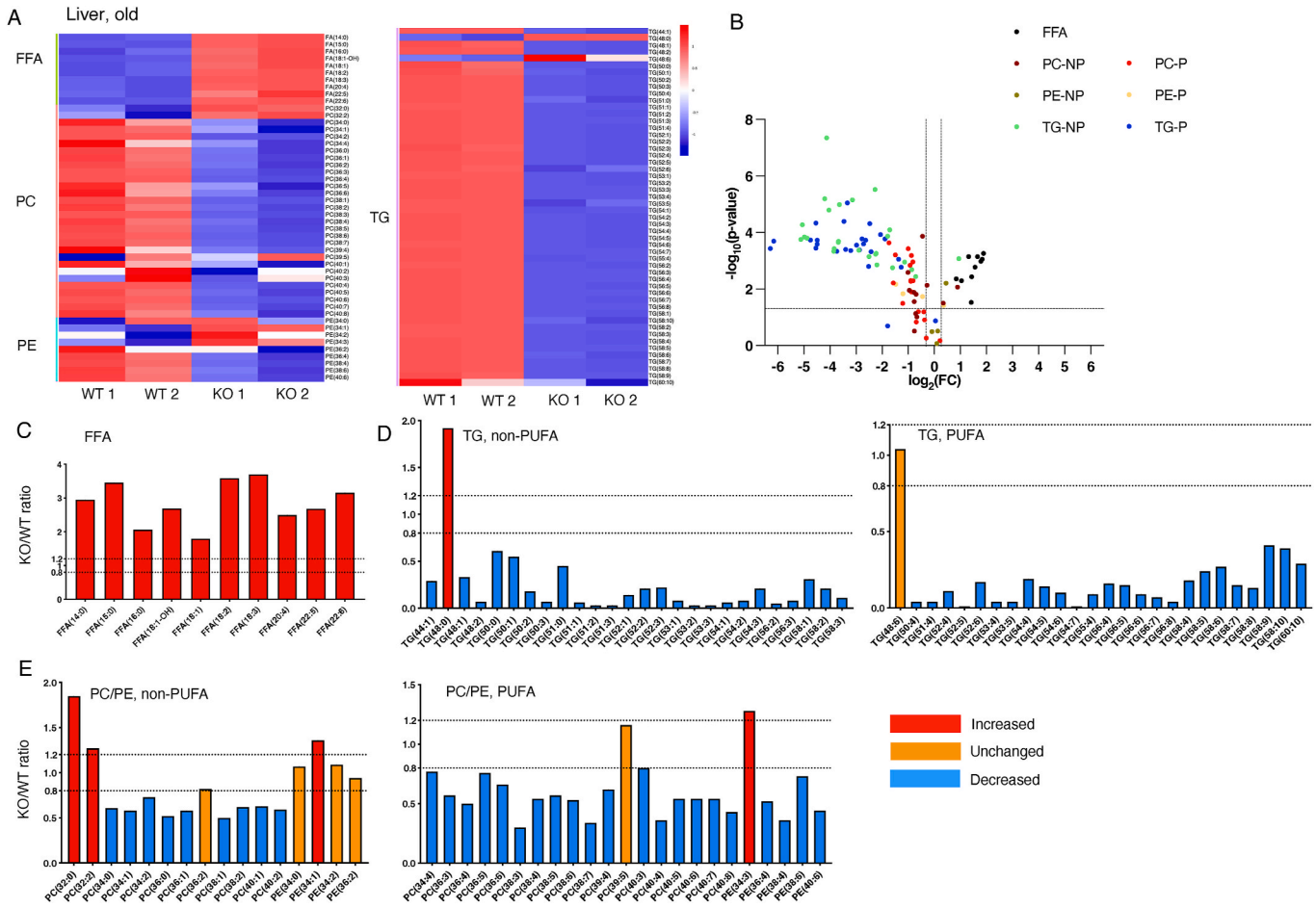

Fig. 2. Lipidomic analysis in old mice livers from WT and L2KO mice

Livers were extracted from six-month-old mice and analyzed using LC-MS/MS. A: Heatmap of all the lipids tested. All data were subjected to log transformation (base 10), mean-centered, and divided by the standard deviation of each variable. B: The volcano map of lipids classified based on unsaturation levels. Vertical dashed lines indicate fold-changes of 0.8 or 1.2, and the horizontal dashed lines indicate P = 0.05 based on Student's *t*-test. C–E: Fold changes of each FFA (C), non-PUFA-TG (D, left panel), PUFA-TG (D, right panel), non-PUFA-PC/PE (E, left panel), and PUFA-PC/PE (E, right panel).

to its role of systemic fatty acid transport.

4.2.1. FFA (young plasma)

In contrast to the increase in FFAs observed in the L2KO mice livers, FFAs in the plasma from L2KO mice significantly decreased compared to those of WT mice at three months (Fig. 3A–B). We identified seven FFA species, including four PUFAs: linolenic acid (18:3), arachidonic acid (20:4), docosapentaenoic acid (DPA) (22:5), and DHA (22:6), all of which had a fold change of less than 0.5 in the KO/WT young plasma (Fig. 3C). Particularly, PUFAs such as DPA (22:5) and DHA (22:6) in the plasma from old L2KO mice significantly decreased to less than 20 % of those in WT mice. This result may imply the potential consumption of FFAs in the peripheral tissues.

4.2.2. TG (young plasma)

TG decreased in young L2KO mice plasma, similar to the results observed in the liver (Fig. 3A–B). We detected 25 TG species, consisting of 10 non-PUFA-TGs and 15 PUFA-TGs (Fig. 3D). All non-PUFA-TGs showed reductions compared to those in WT mice, whereas 9 of 15 (60 %) PUFA-TGs were reduced, indicating that non-PUFA-TGs were more likely to decrease in L2KO mice plasma.

4.2.3. PC/PE (young plasma)

Of the 34 PC/PE species detected in the L2KO mice plasma, including 20 PUFA-PC/PEs and 14 non-PUFA-PC/PEs, 30 of 34 (88.2 %) exhibited no significant changes compared to WT mice (Fig. 3A–B, E).

4.2.4. FFA (old plasma)

In the old L2KO mice plasma, we observed a significant decrease in FFA compared to control WT mice (Fig. 4A–B). We detected seven FFA species. The decline in FFA content was more pronounced in old L2KO mice plasma than that in young L2KO mice (Fig. 4C). While FFA (16:0) in the old L2KO mice plasma decreased to 50 % of that in WT mice, the levels of free PUFAs such as DPA (22:5) and DHA (22:6) were less than 20 % of that in WT mice.

4.2.5. TG (old plasma)

In the old L2KO mice plasma, we observed a pronounced decrease in TGs compared to WT mice (Fig. 4A–B). A total of 34 TG species, including 16 PUFA-TGs and 18 non-PUFA-TGs, were detected in the old mice plasma (Fig. 4D). While some TG species remained relatively unchanged, most (25 out of 34, 73.5 %) significantly decreased compared to that in WT mice.

4.2.6. PC/PE (old plasma)

In old L2KO mice plasma, 32 PC/PE species were detected, including 21 PUFA-PC/PEs and 11 non-PUFA-PC/PEs, both of which significantly decreased compared to that in WT mice. Among the detected species, 7 out of 11 non-PUFA PC/PEs in old L2KO mice plasma decreased to less than 80 % of the WT mice levels, in contrast to the unchanged PC/PEs in

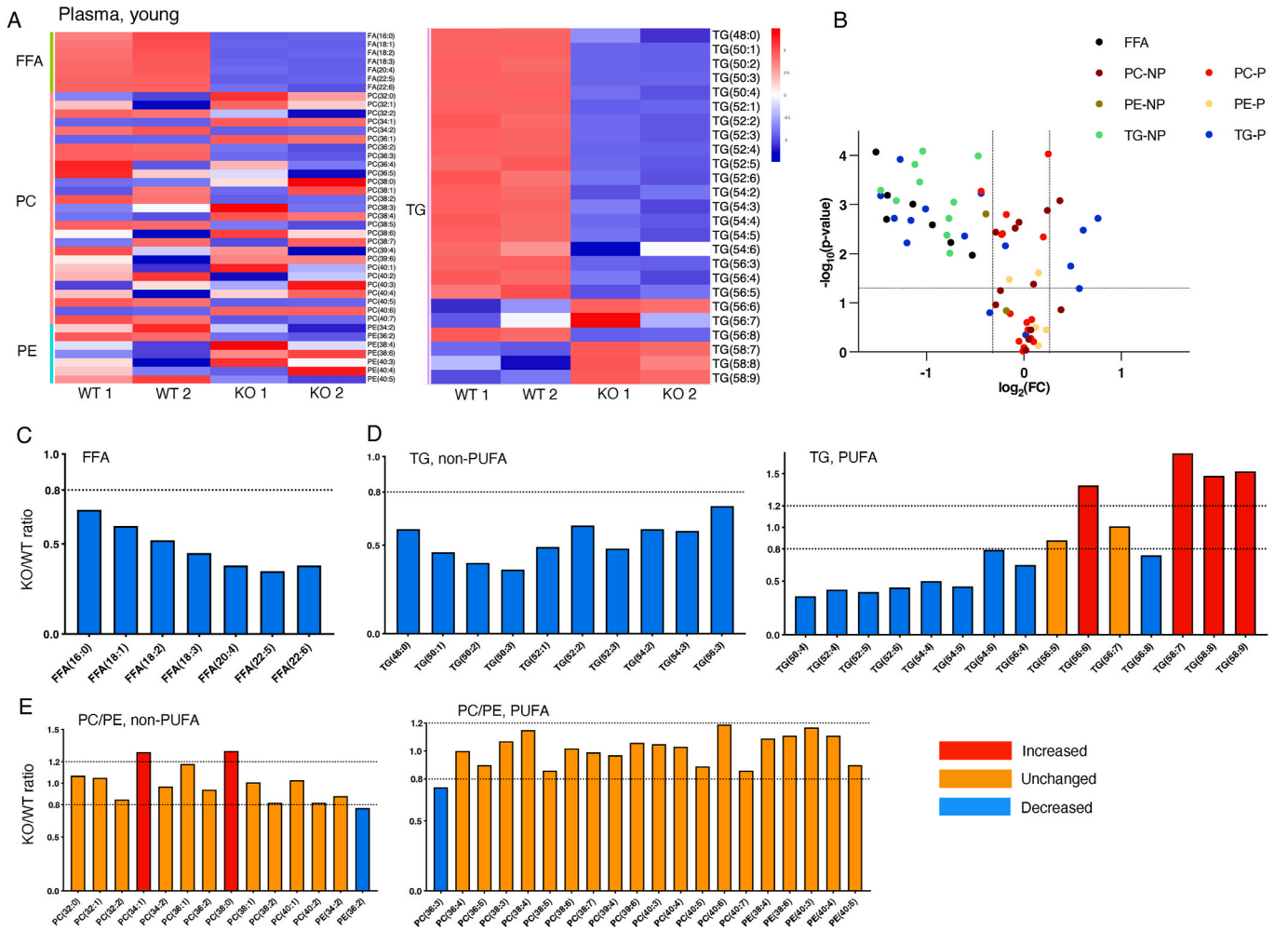

Fig. 3. Lipidomic analysis in young mice plasma from WT and L2KO mice
Plasma was extracted from three-month-old mice and analyzed using LC-MS/MS. A: Heatmap of all the lipids tested. All data were subjected to log transformation (base 10), mean-centered, and divided by the standard deviation of each variable. B: The volcano map of lipids classified based on unsaturation levels. Vertical dashed lines indicate fold-changes of 0.8 or 1.2, and the horizontal dashed lines indicate P = 0.05 based on Student's *t*-test. C–E: Fold changes of each FFA (C), non-PUFA-TG (D, left panel), PUFA-TG (D, right panel), non-PUFA-PC/PE (E, left panel), and PUFA-PC/PE (E, right panel).

young L2KO mice plasma (Fig. 4E, left panel). We also observed that 90.5 % of PUFA-PC/PEs decreased in old L2KO mice plasma (Fig. 4E, right panel).

Thus, the plasma TG levels decreased in L2KO mice, and at the old age PC/PE also decreased similar to the result of liver. However, the plasma FFA levels was downregulated in L2KO mice.

4.3. Lipidomic analysis in the retina

We examined lipid compositions in the retina of L2KO and WT mice and detected some changes in FFA and PC/PE levels (Fig. 5A–B). TG species were not detected, likely because of their low quantity in the neural retina.

4.3.1. FFA (young retina)

We detected seven FFA species in the retina from young L2KO and WT mice (Fig. 5C). Among these, 3 of 7 species (43 %): arachidonic acid (20:4), DHA (22:6), and tetracosanoic acid (24:0), showed more than a 20 % increase.

4.3.2. PC/PE (young retina)

We detected 31 PC/PE species in the retina, consisting of 18 PUFA-PC/PEs and 13 non-PUFA-PC/PE species (Fig. 5D). Among these, 7 of 13 (53.8 %) non-PUFAs and 5 of 18 (27.8 %) PUFA-PC/PEs decreased to less than 90 % of that in WT mice, indicating that non-PUFA-PC/PEs were more likely to be reduced at a young age in the L2KO mice retina.

4.3.3. FFA (old retina)

A total of 6 FFA species were detected in the old mice retina (Fig. 6A–C). Similar to the results in the young mice retina, 5 out of 6 FFAs exhibited an increase in the old L2KO mice retina compared to that in WT mice.

4.3.4. PC/PE (old retina)

A total of 31 PC/PE species were detected in the retinas of L2KO and WT mice, consisting of 18 PUFA-PC/PEs and 13 non-PUFA-PC/PE species (Fig. 6A–B, D). Among these, 6 out of 13 (46 %) non-PUFAs and 7 out of 18 (39 %) PUFA-PC/PEs decreased to less than 90 % of those in the WT mice in the old L2KO mice retina, suggesting that a greater number of PC/PE species decreased with age in the L2KO mice retina.

5. Discussion

In this study, we elucidated the lipidomic profiles of the liver, plasma, and retina of L2KO mice. The contrasting behavior of FFA, which increased in the liver and retina but decreased in the plasma, may

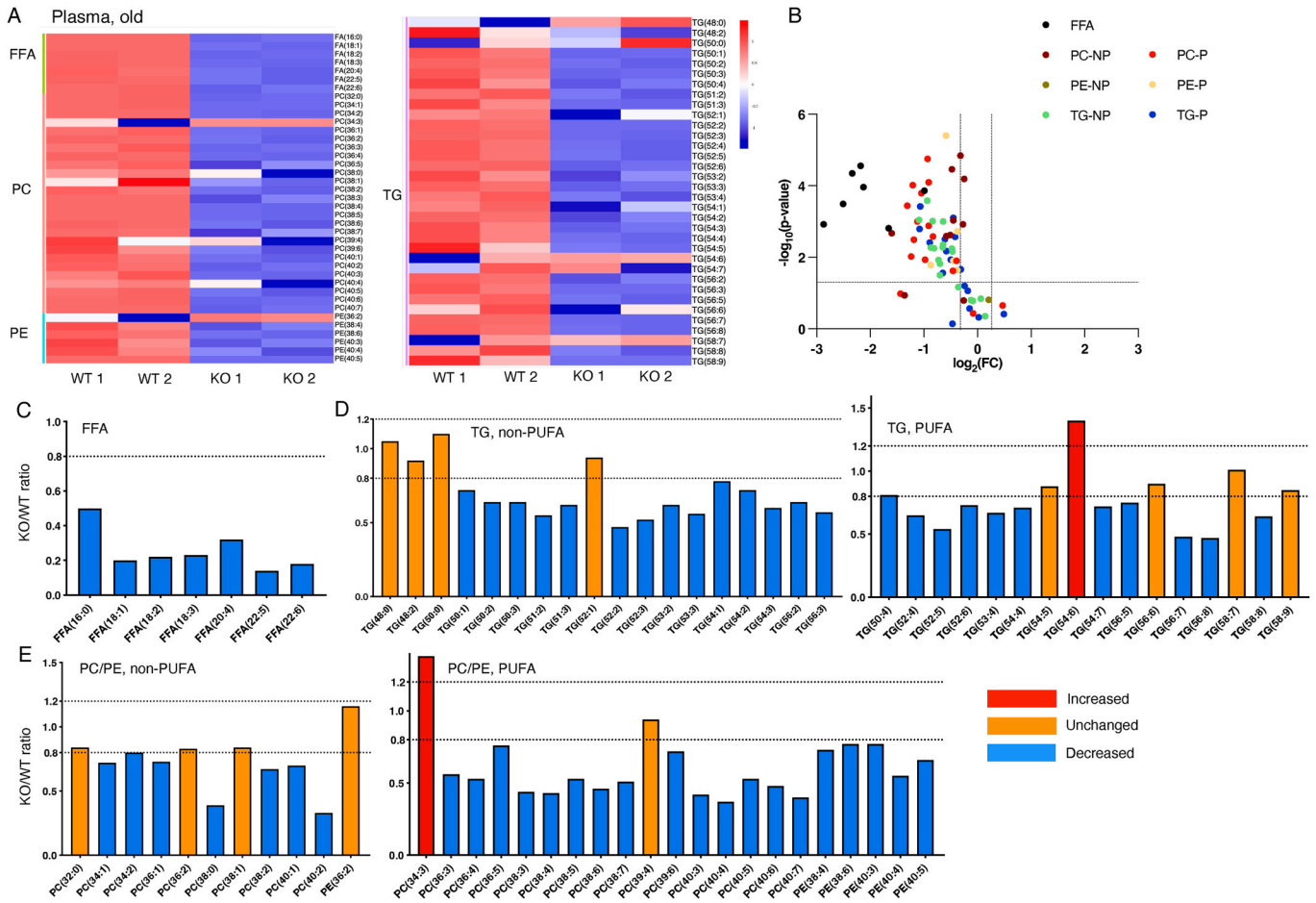

Fig. 4. Lipidomic analysis in old mice plasma from WT and L2KO mice

Plasma was extracted from six-month-old mice and analyzed using LC-MS/MS. A: Heatmap of all the lipids tested. All data were subjected to log transformation (base 10), mean-centered, and divided by the standard deviation of each variable. B: The volcano map of lipids classified based on unsaturation levels. Vertical dashed lines indicate fold-changes of 0.8 or 1.2, and the horizontal dashed lines indicate P = 0.05 based on Student's *t*-test. C–E: Fold changes of each FFA (C), non-PUFA-TG (D, left panel), PUFA-TG (D, right panel), non-PUFA-PC/PE (E, left panel), and PUFA-PC/PE (E, right panel).

suggest an increased local demand for FFA that could serve as an energy source via beta-oxidation. This hypothesis is supported by the observation that TGs and PC/PEs decreased in the peripheral tissues, which may have been consumed for beta-oxidation.

Autophagy is essential for renewal and self-maintenance and provides materials for energy production [15]. Basal autophagy operates consistently at a low level, not only during starvation but also between meals, providing steady energy, particularly in organs such as the liver [16,17]. Its impact on energy metabolism is significant, influencing the three major nutrient metabolic pathways: protein, carbohydrate, and lipid metabolism [15,18–24]. In a previous study, L2KO mice showed a high energy expenditure, resulting in a resistance to high-fat-diet-induced obesity [25]. Therefore, significant changes in fatty acid compositions in this study may be attributed to an increased energy consumption, as FFA is used as primary steady-state energy source in peripheral tissues [26–28]. In contrast to the results in the liver and retina, FFA species in the plasma significantly decreased in L2KO mice. This may have occurred from an upregulated uptake in the peripheral tissues or a limited release from adipose tissues. Moreover, the depletion of plasma FFA was accelerated in old L2KO mice. A previous study, which showed an increased energy expenditure in L2KO mice [25], would support the hypothesis that plasma FFA may have been taken up by peripheral tissues although future studies should clarify the detailed mechanism behind this.

Given the decreased plasma FFA levels, higher FFA levels in the L2KO liver may be caused by an enhanced catabolism of TGs. TGs in liver lipid droplets can be degraded to obtain more FFAs when cells need to supplement their energy sources. Our results showed that TG levels significantly decreased in the L2KO liver. The TG decline in L2KO mice plasma primarily affected non-PUFA-TGs at a young age and then impacted both PUFA- and non-PUFA-TGs at an old age. This shift may be explained as follows: non-PUFAs are supposed to serve as an energy source rather than PUFA because non-PUFAs are more suitable for beta-oxidation [29]. However, if the energy crisis was sustained for a long period, PUFA-TGs also decreased. We assumed this decrease in PUFA-TGs resulted from its degradation to serve as an energy source; however, further investigations are required to shed light upon the reduction in PUFA-TGs L2KO mice. Moreover, a considerable proportion of TGs in the liver of old L2KO mice decreased to even less than 0.1-fold that of aged WT mice, indicating that the lipid storage was almost diminished. This might have contributed to loss of TG in L2KO mice plasma. This deletion of lipid storage in LAMP2 KO mice might have been induced by lipolysis. Liu et al. found that lipid droplets in aged mice were associated with reduced expression of lipolysis enzyme such as adipose triglyceride lipase and hormone-sensitive lipase [30]. Therefore, in our study, LAMP2 deficiency may have caused TG depletion in the liver, potentially due to the lipolysis with upregulated lipolysis enzymes.

PC/PEs are essential components of cellular membranes and regulate lipid and energy metabolism throughout the body [31]. Therefore, changes in PC/PEs in old L2KO mice may also be considered as a result of increased energy demand. In both the liver and plasma, changes in

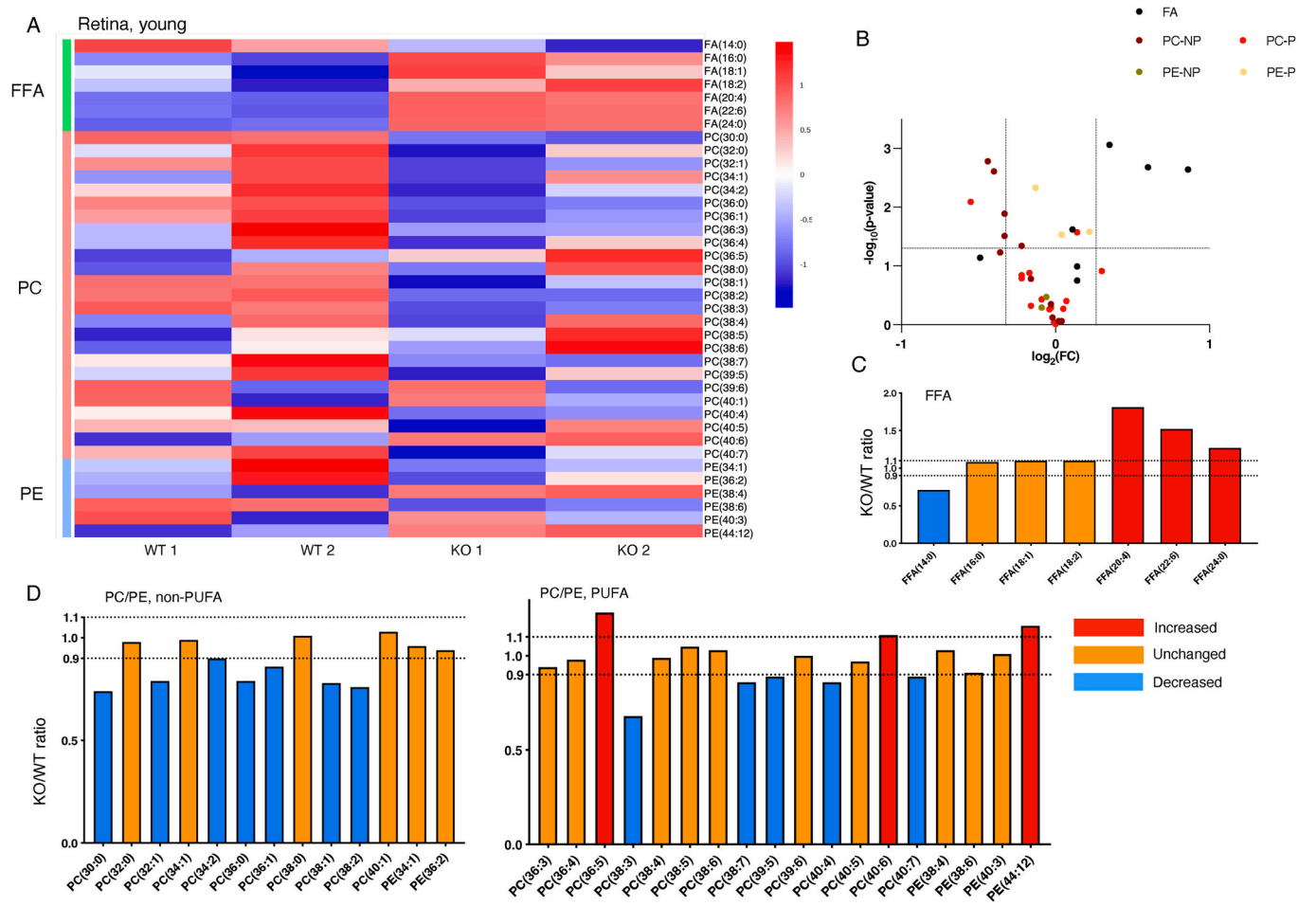

Fig. 5. Lipidomic analysis in young mice retina from WT and L2KO mice
Retina was extracted from three-month-old mice and analyzed using LC-MS/MS. A: Heatmap of all the lipids tested. All data were subjected to log transformation (base 10), mean-centered, and divided by the standard deviation of each variable. B: The volcano map of lipids classified based on unsaturation levels. Vertical dashed lines indicate fold-changes of 0.9 or 1.1, and the horizontal dashed lines indicate P = 0.05 based on Student's *t*-test. C–D: Fold changes of each FFA (C), non-PUFA-PC/PE (D, left panel), PUFA-PC/PE (D, right panel).

PC/PE levels were limited in L2KO mice at a young age. This may be explained by the high energy consumptions in L2KO mice being primarily compensated by TG catabolism at a young age. However, as TGs were depleted with age, reductions in PC/PE levels became evident, presumably to provide more FFAs in peripheral tissues in L2KO mice.

In the retina, the light-sensitive photoreceptor cells use both glucose and fatty acid beta-oxidation for energy production [32]. The increased FFAs in L2KO mice support an expectation that higher FFAs may be associated with high metabolic energy demand in the retina. TG levels were under the detection limit in the retina; hence, the increased FFAs in the retina may be derived from either phospholipids in the plasma or PC/PE degradation in the retina. As phospholipids and FFAs in L2KO mice plasma were much less detectable compared to those in WT mice, the increased FFAs may have resulted from the degradative pathway of PC/PE in the retina. In young L2KO mice retina, PC/PE levels were not affected much although some non-PUFA-PC/PEs decreased. However, as the mice aged, FFAs increased significantly in L2KO mice, suggesting that PC/PE may have been used for beta-oxidation, as observed in the liver.

The decrease of PC/PE affected both non-PUFAs and PUFAs such as DPA and DHA in L2KO mice at an older age. DHA plays a crucial role in maintaining retinal homeostasis [33]. DHA intake regulates the maturation and survival of photoreceptor cells [34–36] and its deficiency is associated with impaired visual function and development [37–39]. Therefore, we analyzed the source of increased free DHA in L2KO mice retinas. PCs were categorized into likely- or unlikely DHA-containing PC based on the composition analysis of the fatty acid chains (Table S1). In the retina, DHA is known to be incorporated into the retinal pigment epithelium as phospholipids, converted to free DHA, and transferred to photoreceptors. Therefore, we initially considered that the elevated free DHA in the retina may have originated from the plasma. However, at an older age, PC/PE was almost depleted in L2KO mice plasma, leading us to consider that free DHA may be supplied from phospholipid degradation within photoreceptors. Consistently, the ratio of L2KO/WT in likely DHA-containing PC was smaller than that in unlikely DHA-containing PC. Therefore, a portion of the increased DHA in the old L2KO mice retina may have been catabolized from DHA-containing PC within the retina itself. Further studies are required to explore this subject.

In addition to the aforementioned fatty acid results, we observed an increase in cholesterol sulfate levels in the liver and retina of L2KO mice (Table S2). Our findings are consistent with those of previous studies showing that LAMP2 deficiency caused lysosomal cholesterol to be stored via inhibiting the late endosome/lysosome cholesterol transport pathway [40,41]. The increase in cholesterol sulfate contrasted with the decrease in TGs and PC/PE. Both fatty acids and cholesterol constitute the cellular membrane and can serve as an energy source. This differential behavior of fatty acids and cholesterol sulfate suggests an imbalance in the membrane-lipid distribution in the pathology of LAMP2 deficiency.

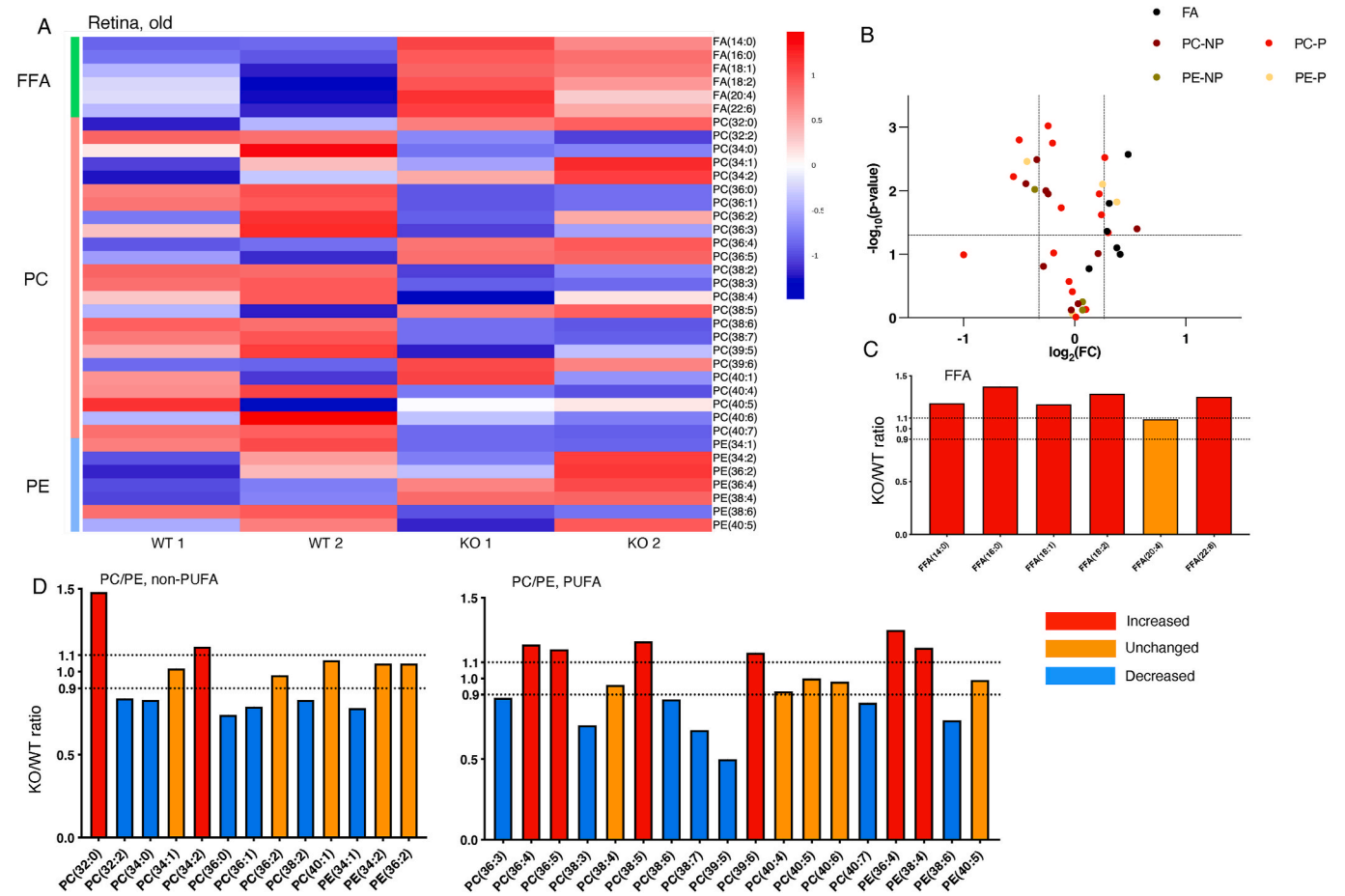

Fig. 6. Lipidomic analysis in old mice retina from WT and L2KO mice

Retina was extracted from six-month-old mice and analyzed using LC-MS/MS. A: Heatmap of all the lipids tested. All data were subjected to log transformation (base 10), mean-centered, and divided by the standard deviation of each variable. B: The volcano map of lipids classified based on unsaturation levels. Vertical dashed lines indicate fold-changes of 0.9 or 1.1, and the horizontal dashed lines indicate P = 0.05 based on Student's *t*-test. C–D: Fold changes of each FFA (C), non-PUFA-PC/PE (D, left panel), PUFA-PC/PE (D, right panel).

There are several limitations in this study. In the LC-MS/MS data analyzed by Kyushu Pro search, we did not determine each fatty acid constituting PC/PE or TG. Therefore, for example, we did not identify which TG could be a source of fatty acids if catabolized. Thus, although we for the first time found notable changes in fatty acid distribution between WT and L2KO mice, we have not clarified the mechanisms responsible for the decreased PC/PE/TG and the increased FFA. We speculate that beta-oxidation would be upregulated to compensate energy crisis in L2KO mice according to the previous study [25]. Further research is required to elucidate the relationship between energy metabolism and fatty acid distribution in L2KO mice.

Our study highlights the significant alterations in fatty acids across the tissues induced by a LAMP2 deficiency. LC-MS/MS analysis has provided a comprehensive understanding of fatty acid change that has never been discussed before. Further, the energy crisis may underscore the importance of autophagy/lysosome-related pathways in the metabolic regulation of fatty acids. Further research will elucidate the relationship between the fatty acids alteration and histopathology caused by LAMP2 deficiencies.

Funding sources

Japan Society for the Promotion of Science, Grants-in-Aid for Scientific Research: JP21K09702.

Data availability

All data are contained within the manuscript or supplemental information.

CRediT authorship contribution statement

Ziming Xu: Writing – original draft, Visualization, Investigation, Formal analysis, Data curation. **Shoji Notomi:** Writing – original draft, Supervision, Project administration, Investigation, Funding acquisition, Conceptualization. **Guannan Wu:** Investigation. **Yosuke Fukuda:** Formal analysis. **Yusuke Maehara:** Investigation, Formal analysis. **Masatoshi Fukushima:** Investigation, Data curation. **Yusuke Murakami:** Writing – review & editing, Supervision. **Masatomo Takahashi:** Writing – review & editing, Validation. **Yoshihiro Izumi:** Writing – review & editing, Validation. **Koh-Hei Sonoda:** Writing – review & editing, Supervision, Project administration.

Declaration of competing interest

The authors declare that they have no known competing financial interests or personal relationships that could have appeared to influence the work reported in this paper.

Data availability

Data will be made available on request.

Acknowledgments

We thank the supports for LC-MS/MS analysis by Kyushu Pro Search Limited Liability Partnership.

Abbreviations

DD	Danon disease
FFA	Free fatty acid
LAMP2	Lysosome-associated membrane protein-2
LC-MS/MS	Liquid chromatography-tandem mass spectrometry
PC	Phosphatidylcholine
PE	Phosphatidylethanolamine
PUFA	Polyunsaturated fatty acid
TG	Triglyceride
WT	Wild-type

Appendix A. Supplementary data

Supplementary data to this article can be found online at https://doi.org/10.1016/j.bbrep.2024.101822.

References

[1] N. Martinez-Lopez, R. Singh, Autophagy and lipid droplets in the liver, Annu. Rev. Nutr. 35 (2015) 215–237.
[2] G. Cenacchi, V. Papa, V. Pegoraro, R. Marozzo, M. Fanin, C. Angelini, Review: Danon disease: review of natural history and recent advances, Neuropathol. Appl. Neurobiol. 46 (4) (2020) 303–322.
[3] F.R. Prall, A. Drack, M. Taylor, L. Ku, J.L. Olson, D. Gregory, L. Mestroni, N. Mandava, Ophthalmic manifestations of Danon disease, Ophthalmology 113 (6) (2006) 1010–1013.
[4] Y. Tanaka, G. Guhde, A. Suter, E.L. Eskelinen, D. Hartmann, R. Lüllmann-Rauch, P. M. Janssen, J. Blanz, K. von Figura, P. Saftig, Accumulation of autophagic vacuoles and cardiomyopathy in LAMP-2-deficient mice, Nature 406 (6798) (2000) 902–906.
[5] J.L. Schneider, Y. Suh, A.M. Cuervo, Deficient chaperone-mediated autophagy in liver leads to metabolic dysregulation, Cell Metabol. 20 (3) (2014) 417–432.
[6] A. Schneede, C.K. Schmidt, M. Hölttä-Vuori, J. Heeren, M. Willenborg, J. Blanz, M. Domanskyy, B. Breiden, S. Brodesser, J. Landgrebe, K. Sandhoff, E. Ikonen, P. Saftig, E.L. Eskelinen, Role for LAMP-2 in endosomal cholesterol transport, J. Cell Mol. Med. 15 (2) (2011) 280–295.
[7] M. Rothaug, S. Stroobants, M. Schweizer, J. Peters, F. Zunke, M. Allerding, R. D'Hooge, P. Saftig, J. Blanz, LAMP-2 deficiency leads to hippocampal dysfunction but normal clearance of neuronal substrates of chaperone-mediated autophagy in a mouse model for Danon disease, Acta Neuropathol Commun 3 (2015) 6.
[8] S. Notomi, K. Ishihara, N.E. Efstathiou, J.J. Lee, T. Hisatomi, T. Tachibana, E. K. Konstantinou, T. Ueta, Y. Murakami, D.E. Maidana, Y. Ikeda, S. Kume, H. Terasaki, S. Sonoda, J. Blanz, L. Young, T. Sakamoto, K.H. Sonoda, P. Saftig, T. Ishibashi, J.W. Miller, G. Kroemer, D.G. Vavvas, Genetic LAMP2 deficiency accelerates the age-associated formation of basal laminar deposits in the retina, Proc. Natl. Acad. Sci. U. S. A. 116 (47) (2019) 23724–23734.
[9] K. Kaarniranta, J. Blasiak, P. Liton, M. Boulton, D.J. Klionsky, D. Sinha, Autophagy in age-related macular degeneration, Autophagy 19 (2) (2023) 388–400.
[10] A. Tsujikawa, K. Takahashi, R. Obata, T. Iida, Y. Yanagi, H. Koizumi, H. Yamashita, F. Shiraga, T. Sakamoto, Dry age-related macular degeneration in the Japanese population, Jpn. J. Ophthalmol. 66 (1) (2022) 8–13.
[11] H. Liu, A. Javaheri, R.J. Godar, J. Murphy, X. Ma, N. Rohatgi, J. Mahadevan, K. Hyrc, P. Saftig, C. Marshall, M.L. McDaniel, M.S. Remedi, B. Razani, F. Urano, A. Diwan, Intermittent fasting preserves beta-cell mass in obesity-induced diabetes via the autophagy-lysosome pathway, Autophagy 13 (11) (2017) 1952–1968.
[12] K. Tanabe, C. Hayashi, T. Katahira, K. Sasaki, K. Igami, Multiblock metabolomics: an approach to elucidate whole-body metabolism with multiblock principal component analysis, Comput. Struct. Biotechnol. J. 19 (2021) 1956–1965.
[13] A.M. Minihane, J.A. Lovegrove, 5 - health benefits of polyunsaturated fatty acids (PUFAs), in: C. Williams, J. Buttriss (Eds.), Improving the Fat Content of Foods, Woodhead Publishing, 2006, pp. 107–140.
[14] E. Trefts, M. Gannon, D.H. Wasserman, The liver, Curr. Biol. 27 (21) (2017) R1147–r1151.
[15] P.W. Lin, M.L. Chu, H.S. Liu, Autophagy and metabolism, Kaohsiung J. Med. Sci. 37 (1) (2021) 12–19.
[16] A. Kuma, M. Hatano, M. Matsui, A. Yamamoto, H. Nakaya, T. Yoshimori, Y. Ohsumi, T. Tokuhisa, N. Mizushima, The role of autophagy during the early neonatal starvation period, Nature 432 (7020) (2004) 1032–1036.
[17] N. Mizushima, A. Yamamoto, M. Matsui, T. Yoshimori, Y. Ohsumi, In vivo analysis of autophagy in response to nutrient starvation using transgenic mice expressing a fluorescent autophagosome marker, Mol. Biol. Cell 15 (3) (2004) 1101–1111.
[18] R. Singh, A.M. Cuervo, Autophagy in the cellular energetic balance, Cell Metabol. 13 (5) (2011) 495–504.
[19] J.J. Lum, D.E. Bauer, M. Kong, M.H. Harris, C. Li, T. Lindsten, C.B. Thompson, Growth factor regulation of autophagy and cell survival in the absence of apoptosis, Cell 120 (2) (2005) 237–248.
[20] E. Arias, A.M. Cuervo, Chaperone-mediated autophagy in protein quality control, Curr. Opin. Cell Biol. 23 (2) (2011) 184–189.
[21] J.P. Schellens, H. Vreeling-Sindelárová, P.J. Plomp, A.J. Meijer, Hepatic autophagy and intracellular ATP. A morphometric study, Exp. Cell Res. 177 (1) (1988) 103–108.
[22] C.M. Schworer, J.R. Cox, G.E. Mortimore, Alteration of lysosomal density by sequestered glycogen during deprivation-induced autophagy in rat liver, Biochem. Biophys. Res. Commun. 87 (1) (1979) 163–170.
[23] S.A. Kalamidas, O.B. Kotoulas, Glycogen autophagy in newborn rat hepatocytes, Histol. Histopathol. 15 (4) (2000) 1011–1018.
[24] C. Ebato, T. Uchida, M. Arakawa, M. Komatsu, T. Ueno, K. Komiya, K. Azuma, T. Hirose, K. Tanaka, E. Kominami, R. Kawamori, Y. Fujitani, H. Watada, Autophagy is important in islet homeostasis and compensatory increase of beta cell mass in response to high-fat diet, Cell Metabol. 8 (4) (2008) 325–332.
[25] M. Yasuda-Yamahara, S. Kume, K. Yamahara, J. Nakazawa, M. Chin-Kanasaki, H. Araki, S. Araki, D. Koya, M. Haneda, S. Ugi, H. Maegawa, T. Uzu, Lamp-2 deficiency prevents high-fat diet-induced obese diabetes via enhancing energy expenditure, Biochem. Biophys. Res. Commun. 465 (2) (2015) 249–255.
[26] J.S. Joyal, Y. Sun, M.L. Gantner, Z. Shao, L.P. Evans, N. Saba, T. Fredrick, S. Burnim, J.S. Kim, G. Patel, A.M. Juan, C.G. Hurst, C.J. Hatton, Z. Cui, K. A. Pierce, P. Bherer, E. Aguilar, M.B. Powner, K. Vevis, M. Boisvert, Z. Fu, E. Levy, M. Fruttiger, A. Packard, F.A. Rezende, B. Maranda, P. Sapieha, J. Chen, M. Friedlander, C.B. Clish, L.E. Smith, Retinal lipid and glucose metabolism dictates angiogenesis through the lipid sensor Ffar1, Nat. Med. 22 (4) (2016) 439–445.
[27] Z. Fu, T.S. Kern, A. Hellström, L.E.H. Smith, Fatty acid oxidation and photoreceptor metabolic needs, J. Lipid Res. 62 (2021) 100035.
[28] G.D. Lopaschuk, J.R. Ussher, C.D. Folmes, J.S. Jaswal, W.C. Stanley, Myocardial fatty acid metabolism in health and disease, Physiol. Rev. 90 (1) (2010) 207–258.
[29] H. Schulz, Fatty acid oxidation, in: W.J. Lennarz, M.D. Lane (Eds.), Encyclopedia of Biological Chemistry, second ed., Academic Press, Waltham, 2013, pp. 281–284.
[30] C. Liu, C. Wu, S. Zhang, Z. Lv, Contribution of impaired autophagy, mitochondrial dysfunction and abnormal lipolysis to epididymal aging in mice, Exp. Gerontol. 195 (2024) 112528.
[31] J.N. van der Veen, J.P. Kennelly, S. Wan, J.E. Vance, D.E. Vance, R.L. Jacobs, The critical role of phosphatidylcholine and phosphatidylethanolamine metabolism in health and disease, Biochim. Biophys. Acta Biomembr. 1859 (9 Pt B) (2017) 1558–1572.
[32] R.V. Rajala, T.W. Gardner, Burning fat fuels photoreceptors, Nat. Med. 22 (4) (2016) 342–343.
[33] N.G. Bazan, A. Asatryan, Docosahexaenoic acid (DHA) in stroke, Alzheimer's disease, and blinding retinal degenerations: coping with neuroinflammation and sustaining cell survival, OCL 18 (4) (2011) 208–213.
[34] B. Jastrzebska, A. Debinski, S. Filipek, K. Palczewski, Role of membrane integrity on G protein-coupled receptors: rhodopsin stability and function, Prog. Lipid Res. 50 (3) (2011) 267–277.
[35] B.G. Jeffrey, M. Neuringer, Age-related decline in rod phototransduction sensitivity in rhesus monkeys fed an n-3 fatty acid-deficient diet, Invest. Ophthalmol. Vis. Sci. 50 (9) (2009) 4360–4367.
[36] R.M. Benolken, R.E. Anderson, T.G. Wheeler, Membrane fatty acids associated with the electrical response in visual excitation, Science 182 (4118) (1973) 1253–1254.
[37] R. Uauy, D.R. Hoffman, P. Peirano, D.G. Birch, E.E. Birch, Essential fatty acids in visual and brain development, Lipids 36 (9) (2001) 885–895.
[38] J.P. SanGiovanni, E.Y. Chew, The role of omega-3 long-chain polyunsaturated fatty acids in health and disease of the retina, Prog. Retin. Eye Res. 24 (1) (2005) 87–138.
[39] H. Shindou, H. Koso, J. Sasaki, H. Nakanishi, H. Sagara, K.M. Nakagawa, Y. Takahashi, D. Hishikawa, Y. Iizuka-Hishikawa, F. Tokumasu, H. Noguchi, S. Watanabe, T. Sasaki, T. Shimizu, Docosahexaenoic acid preserves visual function by maintaining correct disc morphology in retinal photoreceptor cells, J. Biol. Chem. 292 (29) (2017) 12054–12064.
[40] Y. Meng, S. Heybrock, D. Neculai, P. Saftig, Cholesterol handling in lysosomes and beyond, Trends Cell Biol. 30 (6) (2020) 452–466.
[41] J. Li, S.R. Pfeffer, Lysosomal membrane glycoproteins bind cholesterol and contribute to lysosomal cholesterol export, Elife 5 (2016).